5ICEGE
5th International Conference on Earthquake Geotechnical Engineering
January 2011, 10-13 | Santiago, Chile
Paper No. RSSKL

RANKINE SOLUTION FOR SEISMIC EARTH PRESSURES ON L-SHAPED RETAINING WALLS

Panos KLOUKINAS [1], George MYLONAKIS [2]

ABSTRACT

An exact limit-stress solution is presented for the problem of seismic earth pressures on L-shaped cantilever walls retaining dry cohesionless soil. It is shown that the problem can be analyzed by means of a Rankine stress field in the backfill for an infinite set of geometric and material parameters obeying a transcendental equation in friction angle ϕ. Key to the proposed approach is that the stress characteristics in the soil mass do not intersect the stem of the wall. Consequently, the soil-wall interface is not part of the sliding wedge and the roughness of the wall does not influence the response, as the interface remains bonded. In light of the above, the solution can be obtained analytically, in the realm of plane strain conditions and pseudo-dynamic seismic action in the backfill. The suitability of the popular "virtual vertical back" approach for evaluating active thrusts is confirmed and the corresponding roughness angle $\delta(0)$ is derived in closed form as function of friction angle, backfill inclination and seismic acceleration. It is shown that existing recommendations for $\delta(0)$ in seismic codes are often erroneous – yet may yield predictions on the safe side. Optimization aspects referring to improvement of system stability and corresponding safety factors are investigated. Issues related to the use (or misuse) of the safety factor against overturning are discussed.

Keywords: L-shaped Retaining Wall, Stress Plasticity, Limit Analysis, Rankine , Seismic earth pressures

INTRODUCTION

Cantilever walls of L or inverted T-shape represent a popular type of retaining system, which is widely considered as advantageous over conventional gravity walls for it combines economy and ease in construction and installation. Furthermore, the specific design is particularly rational, as it exploits the stabilizing action of soil weight over the footing slab against both sliding and overturning. A contradictory issue in the literature relates to the calculation of active thrust, assumed to be acting on a virtual wall back, which is usually taken as the vertical plane passing through the heel of the wall, under a pertinent mobilized roughness on this plane (Trenter, 2004; O'Sullivan and Creed, 2007).

The problem under consideration is presented in Fig. 1: a sloping backfill of dry cohesionless soil is retained by an L - shaped cantilever wall. The system is subjected to plane strain conditions under the combined action of gravity (g) and seismic body forces ($a_h \times g$) and ($a_v \times g$) in the horizontal and vertical direction, respectively. The problem parameters are: wall height H, heel width b, footing width B, wall thickness t, wall unit weight γ_w, wall roughness δ_w, soil unit weight γ and soil friction angle ϕ. The pseudo-dynamic seismic angle resulting from the gravitational and the inertial body forces, shown in Fig.

[1] Ph.D Candidate, Department of Civil Engineering, University of Patras, Greece, e-mail: pkloukin@upatras.gr
[2] Associate Professor, Department of Civil Engineering, University of Patras, Greece, e-mail: mylo@upatras.gr

1, is $\psi_e = \tan^{-1}[a_h/(1-a_v)]$. The problem is treated by means of a stress limit analysis method in the realm of plasticity theory. It will be shown that the solution can be obtained as a Rankine stress field.

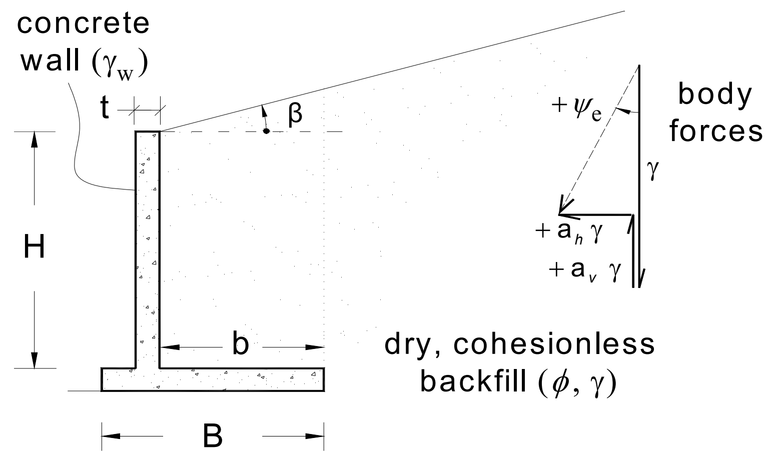

Figure 1. The problem under consideration

STRESS LIMIT ANALYSIS

General approximate solution

The herein-reported solution is based on the stress limit analysis approach of Mylonakis et al (2007), which makes use of discontinuous stress fields, like the one shown in Fig. 2. In this solution the soil mass is divided into three regions: Zone A (Rankine Zone) located near the free surface of the semi-finite slope; Zone B (Rankine Zone) which satisfies the stress boundary condition on the soil-wall interface; Zone C – a transition region between regions A and B.

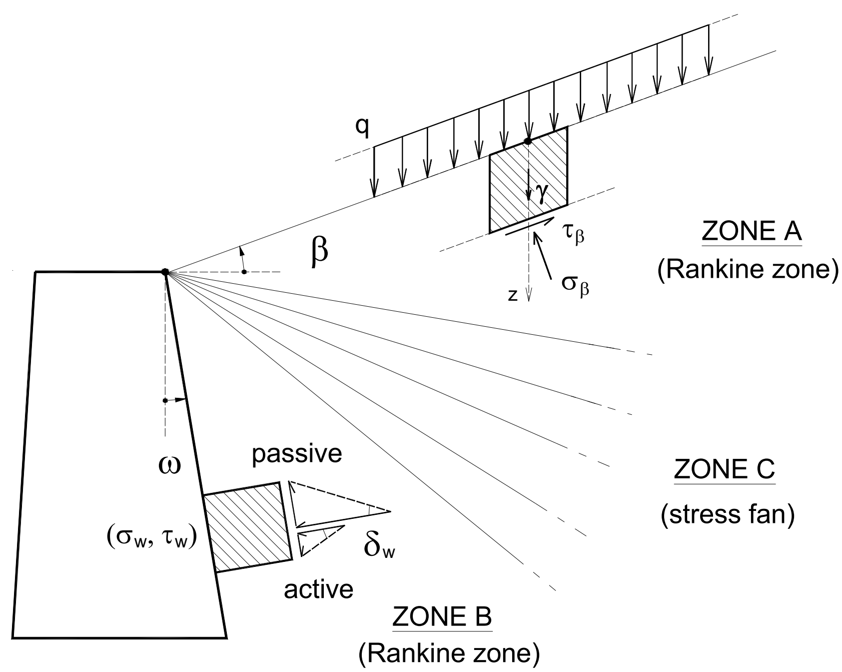

Figure 2. Discontinuous stress field in the case of a gravity wall (After Mylonakis et al., 2007)

The boundary condition on the wall (Zone B) imposes two restrictions: *First* it enforces the failure criterion at the soil-wall interface (i.e. $\tau_w = \sigma_w \tan\delta_w$) as the particular surface is a failure plane; *Second* it prescribes the direction of the coaxial shear traction on the wall surface, that points in the same direction as the velocity vector of the retained soil mass (which is obviously different in the active and the passive case). As to the transition Zone C, a logarithmic stress fan is adopted, which is an exact solution for a weightless material, yet only approximate for material with weight. The expression providing the ultimate thrust for active and passive conditions is given by the well known equation (Ebeling & Morison, 1992; Kramer, 1996):

$$P_E = K_{qE}(1-a_v)qH + \frac{1}{2}K_{\gamma E}(1-a_v)\gamma H^2 \tag{1}$$

where,

$$K_{\gamma E} = \frac{\cos(\omega-\beta)\cos(\beta+\psi_e)}{\cos\psi_e \cos\delta_w \cos^2\omega}\left[\frac{1-\sin\phi\cos(\Delta_2-\delta_w)}{1+\sin\phi\cos(\Delta_{1e}+\beta+\psi_e)}\right]\exp(-2\theta_E\tan\phi) \tag{2}$$

$$K_{qE} = K_{\gamma E}\cos\omega / \cos(\omega-\beta) \tag{3}$$

$$\sin\Delta_{1e} = \sin(\beta+\psi_e)/\sin\phi\,,\;\; \sin\Delta_2 = \sin\delta_w/\sin\phi \tag{4}$$

$$2\theta_E = (\Delta_2-\delta_w) - (\Delta_{1e}-\beta) - 2\omega - \psi_e \tag{5}$$

In the above equations, $K_{\gamma E}$ and K_{qE} are earth pressure coefficients pertaining to self-weight and surcharge, respectively; Δ_{1e} and Δ_2 are the corresponding Caquot angles (measured in radians) and θ_E is the rotation angle of the principal planes (and, accordingly, stress characteristics), which is equal to the opening angle of the transition zone. Equations (2) to (5) provide both the active thrust and the passive resistance, provided that a proper sign is used for the friction angle ϕ and the roughness angle δ_w. This merely requires positive δ_w, ϕ for active conditions and negative δ_w, ϕ for passive.

Generalized Rankine theory

In the special case of a vanishing angle θ_E, the three stress fields in Fig. 2 collapse into a simple continuous Rankine zone, which is depicted by the Mohr circle of Fig. 3. In this special case, the exponential term in Eq. (2) vanishes and the equation provides an exact solution of the Rankine type for the generalized problem with earthquake loading. The necessary condition for the validity of this solution is (see Eq. 5):

$$(\Delta_2-\delta_w) - (\Delta_{1e}-\beta) - 2\omega - \psi_e = 0 \tag{6}$$

which, naturally, is satisfied by an infinite combinations of the five governing parameters (i.e. ϕ, δ_w, ω, β and ψ_e). Among them, as special cases, one can identify the classical solutions of the literature, i.e. $\delta_w = \omega = \beta = \psi_e = 0$ and $\delta_w = \beta$, $\omega = \psi_e = 0$. Under these conditions, the solution attains the special forms of Eq. (7) and (8), which are equivalent to the solutions in Rankine (1857) and Terzaghi (1943).

$$K_\gamma = (1-\sin\phi)/(1+\sin\phi) \tag{7}$$

$$K_\gamma = \cos\beta \frac{1-\sin\phi\cos(\Delta_1-\beta)}{1+\sin\phi\cos(\Delta_1+\beta)} \tag{8}$$

From Eq. (6) and the Mohr circle of Fig. 3, it is straightforward to derive the critical values of each of the above parameters as function of the others, to satisfy the generalized Rankine condition. These solutions are given in Eqs. (9) to (12). Equation (9) results directly from condition (6), whereas derivation of Eqs. (10) to (12) requires additional geometric considerations from the stress tensor of Fig. 3.

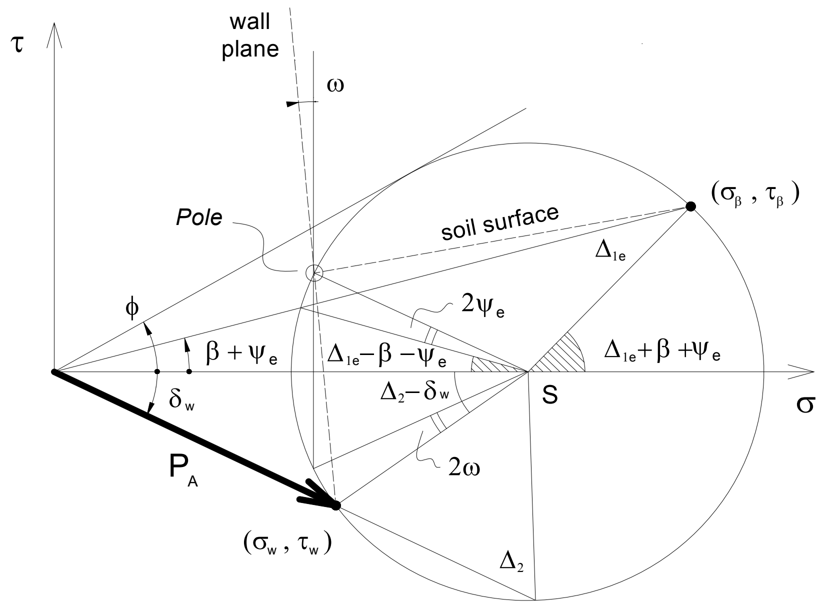

Figure 3 Generalized Rankine stress tensor for earthquake loading

$$\omega_R = \frac{1}{2}\left[(\Delta_2-\delta_w)-(\Delta_{1e}-\beta)-\psi_e\right] \tag{9}$$

$$\beta_R = tan^{-1}\left[\frac{\sin\phi\sin(\Delta_2-\delta_w-2\omega-2\psi_e)}{1-\sin\phi\cos(\Delta_2-\delta_w-2\omega-2\psi_e)}\right]-\psi_e \tag{10}$$

$$\psi_{eR} = tan^{-1}\left[\frac{\sin\phi\sin(\Delta_2-\delta_w-2\omega+2\beta)}{1+\sin\phi\cos(\Delta_2-\delta_w-2\omega+2\beta)}\right]-\beta \tag{11}$$

$$\delta_R = \tan^{-1}\left[\frac{\sin\phi\sin(\Delta_{1e}-\beta+\psi_e+2\omega)}{1-\sin\phi\cos(\Delta_{1e}-\beta+\psi_e+2\omega)}\right] \tag{12}$$

For the simpler case of gravitational loading, the counterparts of Eqs. (9) and (12) can be found in the work of Costet & Sanglerat (1979), whereas an alternative form of equation (12) is given in Chu (1991). The latter solution makes use of the erroneous assumption that the thrust inclination δ_R in Eq. (12) (for ψ_e = 0) can actually develop on the wall plane regardless of the true interface angle δ_w. As a result, the analysis reported in this work violates the failure criterion at the interface and may be incompatible with the kinematics of the problem (Budhu, 2007).

It should be noticed that for every combination of parameters ϕ, δ_w, ω, β and ψ_e satisfying Eqs. (9) – (12), the predictions of Eq. (2) coincide with those of the Mononobe – Okabe equation and other approximate solutions (Chu, 1991; Greco, 1999). This stems from the properties of the Rankine stress field and the associated straight stress characteristics. As a result, the predictions of all methods not only coincide, but they are also exact in the realm of classical plasticity theory. As pointed out by Heyman (1973), the origins of these solutions can be traced back in the pioneering studies of Rankine (1857), Boussinesq (1876) and Levy (1874).

ANALYSIS OF L – SHAPED WALL

Unlike the case of gravity walls where the generalized Rankine condition arises only for specific combinations of the five governing parameters of the problem, specified by Eq. (6), in the case of L-shaped cantilever walls the theory has much wider applicability. Indeed, when the heel of the wall is sufficiently long, the stress characteristics (i.e the conjugate failure planes from Mohr circle, here front reported as α and β - characteristic) in the backfill do not intersect the stem of the wall. Then, the sliding prism is formed entirely in the backfill, as shown in Fig. 4a. As a result, the soil – wall interface is not part of the Rankine zone and does not influence the response for the interface remains bonded and lies out of the failure mechanism.

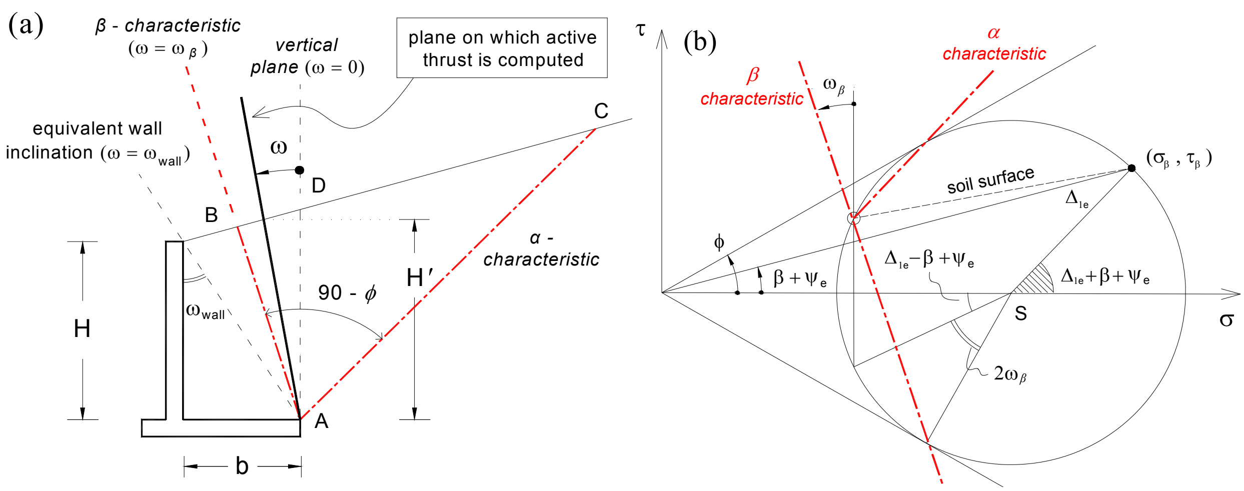

Figure 4. (a) Rankine wedge in the backfill and applicability condition of Rankine solution, (b) Stress tensor and stress characteristics in the retained soil.

From Figure 4a, the geometric condition for the validity of the above Rankine solution is:

$$\omega_\beta \leq \omega_{wall} \quad \text{or, equivalently,} \quad \omega_\beta \leq tan^{-1}\left(b/H\right) \qquad (13)$$

which is tantamount to the criterion provided by Clayton et al. (1993) for the corresponding static problem. The inclination of the β – characteristic can be determined either graphically, from the corresponding Mohr circle (Figure 4b) or, alternatively, from Eq. (9) using $\delta = \phi$; this yields the solution:

$$\omega_\beta = \frac{\pi}{4} - \frac{\phi}{2} - \frac{(\Delta_{1e} - \beta)}{2} - \frac{\psi_e}{2} \qquad (14)$$

For the simple case of gravitational loading ($\psi_e = 0$), Eq. (14) can be found in a number of publications (e.g. Costet & Sanglerat, 1979; Chu, 1991; Clayton et al, 1993). To the best of the authors knowledge, the case of earthquake loading has not been investigated in the past.

In Fig. 5, the minimum required heel length to ensure the validity of the Rankine condition is presented as function of horizontal seismic acceleration a_h and backfill angle, β. It can be clearly seen that the minimum required length is not constant, but decreases with increasing acceleration level. [This is in contrast to the constant value (b > H/3) proposed by a number of seismic provisions including the current Greek Seismic Code, EAK2000]. This decrease in heel length suggests that condition (13) can be satisfied in many cases involving earthquake loading, even if it is not satisfied for the corresponding gravitational loading. As a result, the condition proposed by the Greek code covers a wide range of common cases, except for those associated with small values of slope angle, β.

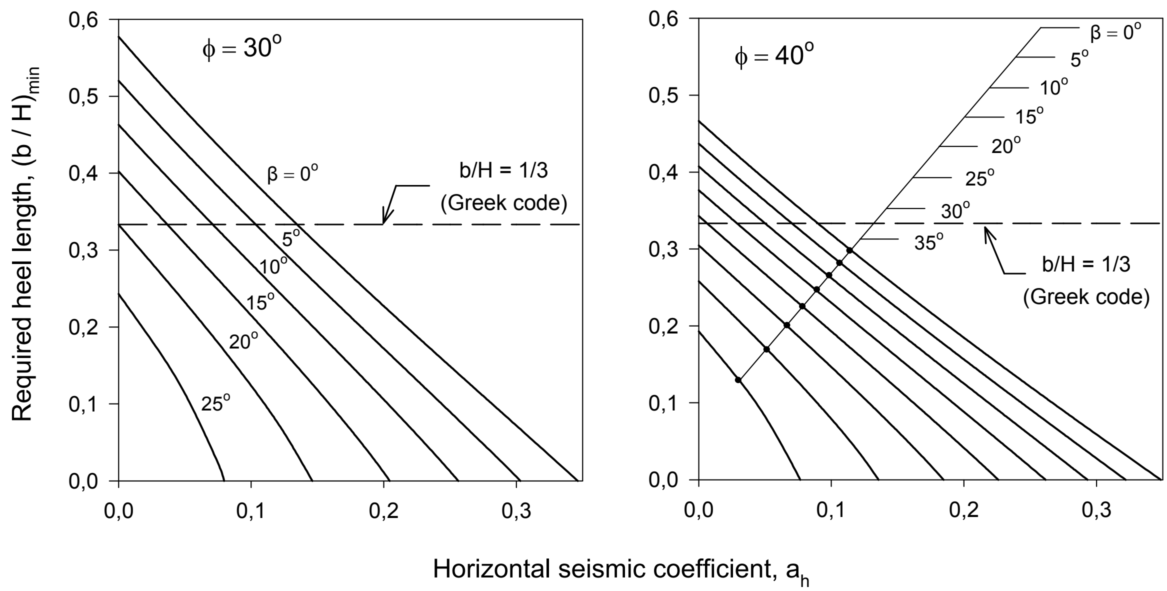

Figure 5. Variation of minimum required heel length with horizontal acceleration coefficient and backfill angle.

For the cases where the Rankine condition is valid, the active earth pressure can be determined from Eqs. (1) – (4) in conjunction with Eq. (12), on any plane (to be referred to hereafter as "virtual back") inclined at an angle ω from vertical (Fig.4), resulting to:

$$K_\gamma = \frac{\cos(\omega - \beta)\cos(\beta + \psi_e)}{\cos\delta(\omega)\cos^2\omega\cos\psi_e}\left[\frac{1 - \sin\phi\cos(\Delta_2 - \delta(\omega))}{1 + \sin\phi\cos(\Delta_{1e} + \beta + \psi_e)}\right] \qquad (15)$$

On this arbitrary plane, the active's thrust inclination $\delta(\omega)$, is given by Eq. (12) for the specific inclination ω. This elucidates that the naive, yet frequently used, assumption of a «soil-to-soil» friction angle equal ϕ

is erroneous (BS8002, 1994; Trenter, 2004, O'Sullivan and Creed, 2007). Only for the case where $\omega = \omega_\beta$, that is when the plane under consideration is parallel to a β-characteristic (Fig. 4), the mobilized friction angle $\delta(\omega)$ is equal to ϕ. Naturally, this is the maximum value that the interface friction angle δ can mobilize.

In light of Fiq. 4, an effective wall height *H'* has to be introduced according to Eq. (16), which, evidently varies with the angle ω of the virtual back.

$$H' = H\left[1+\left(\frac{b}{H}-\tan\omega\right)\frac{\sin\beta\cos\omega}{\cos(\omega-\beta)}\right] \qquad (16)$$

In Figure 6, two extreme cases are presented, corresponding to cases where $\omega = \omega_\beta$ and $\omega = 0$, which have been widely used in the literature (Clayton et al., 1993; Greco, 1999; Trenter, 2004). It is easy to prove that the above options are statically equivalent, as they lead to the same resultant force on the wall (if the body forces in the corresponding hatched soil prisms of Fig. 6a, b are accounted for).

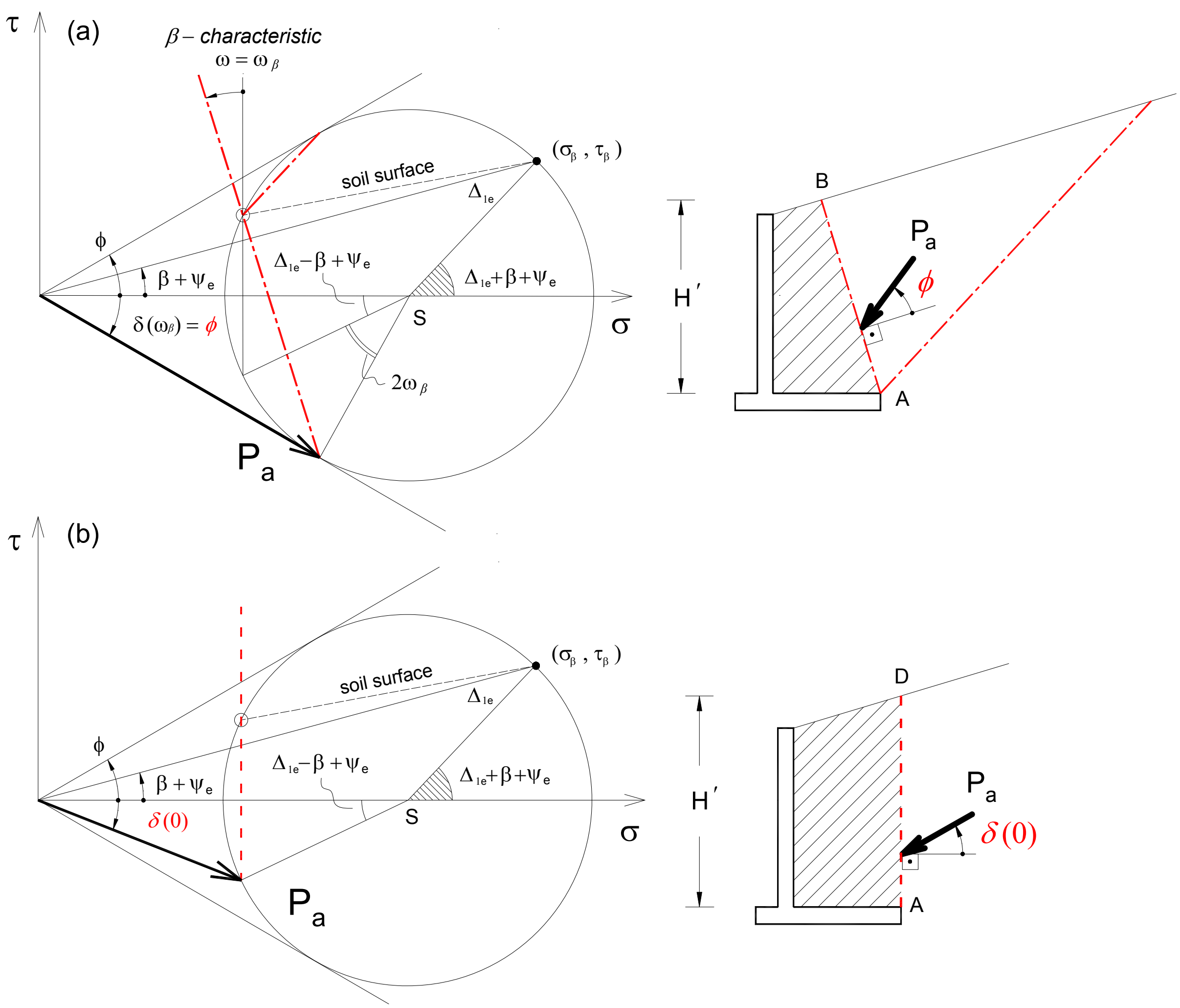

Figure 6. (a) Active thrust on the actual slip line AB (*β*-characteristic) and (b) Active thrust on the vertical virtual back AD.

This is despite the fact that the active thrust P_A, calculated for each case on plane ω is different (Fig. 6a, b). Notwithstanding the last remark, it is preferable to adopt the conventional vertical plane AD, corresponding to ω = 0 as virtual back, for it leads to a simpler geometry (Fig. 6b). Accordingly, Eqs. (17) and (18) are derived for the determination of the magnitude of the thrust and its inclination δ(0):

$$K_\gamma = \frac{\cos\beta\cos(\beta+\psi_e)}{\cos\delta(0)\cos\psi_e}\left[\frac{1-\sin\phi\cos\left(\Delta_{1e}-\beta+\psi_e\right)}{1+\sin\phi\cos\left(\Delta_{1e}+\beta+\psi_e\right)}\right] \tag{17}$$

$$\delta(0) = tan^{-1}\left[\frac{\sin\phi\sin\left(\Delta_{1e}-\beta+\psi_e\right)}{1-\sin\phi\cos\left(\Delta_{1e}-\beta+\psi_e\right)}\right] \tag{18}$$

In Figure 7 results for the mobilized friction angle $\delta(0)$ on the vertical virtual back are presented, as function of horizontal seismic acceleration and slope inclination for soil friction angles $\phi = 30^o$ and 40^o. It can be observed that the virtual back roughness is not always equal to the slope inclination β, but only for the case of gravitational loading (ψ_e = a_h = 0). In presence of seismic action, the roughness increases significantly up to the peak $\delta = \phi$ value, when the β-characteristic becomes vertical ($\omega_\beta = 0$), that is for the same earthquake level for which the required heel length in Fig. 5 vanishes (Note that all the curves are plotted up to the peak value; the following decreasing branch is absent). This suggests that the common assumption $\delta = \beta$ in the seismic codes is precise only for gravitational loading and generally underestimates δ. However, this assumption, although erroneous, yields results on the safety side, as the increase in roughness, forces an increase in stability (through a higher vertical and a lower horizontal component of thrust). Different – yet also erroneous – assumptions for the mobilized δ value can be found in the literature (i.e. BS:8002, $\delta=\phi$ based on the naive assumption of «soil-to-soil» friction; AASHTO LRFD, $\delta=\delta_w$ by an association of the actual soil-wall interface with the vertical virtual back).

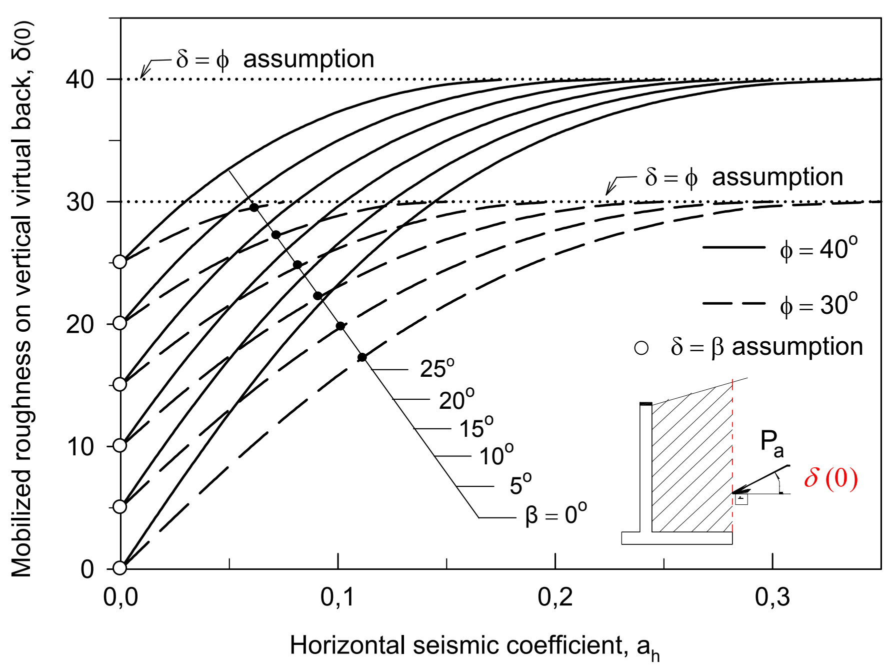

Figure 7. Variation of inclination of active thrust on vertical plane as function of horizontal seismic acceleration and backfill inclination

STABILITY SAFETY FACTORS

Traditionally, stability control of retaining walls is based on safety factors against bearing capacity, sliding and overturning. Of these, only the first two are rationally defined, whereas the safety factor against overturning is known to be erroneous (Greco, 1997). In Figure 8, the equilibrium of forces acting on the retaining wall is presented. Evidently, the total vertical and horizontal forces acting on the wall are compensated by the external reactions N and T acting on the footing. The combination of these two actions, together with the resulting eccentricity e, determines the bearing capacity of the wall, based on classical limit analysis procedures for a strip footing subjected an eccentric and inclined load (e.g. EC7).

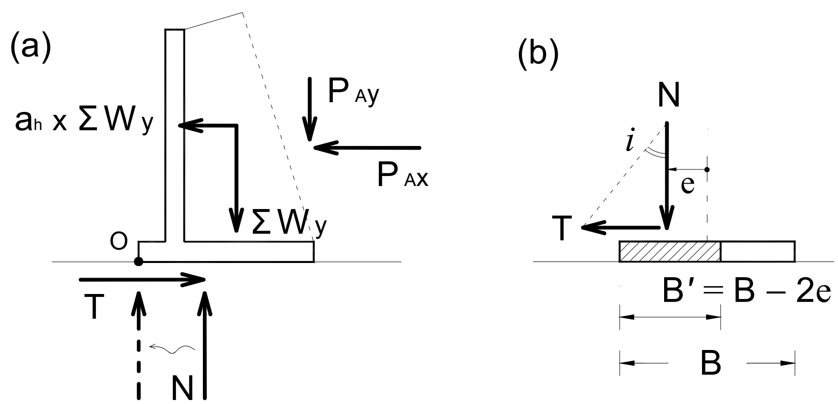

Figure 8. (a) Equilibrium of forces; (b) equivalent centrically loaded footing according to Meyerhof

The safety factors against bearing capacity and sliding are well defined as the ratio of forces N and T over the corresponding ultimate loads. In contrast, the safety factor against overturning is not defined on a rational base; Its calculation assumes a limit state of rotation about the toe O of the wall, which is the point where the vertical reaction N acts (so it generates zero moment with respect to O), since the wall base is not considered to be in contact with the ground. Then, the moments of the remaining forces acting on the wall are compared upon classification (in an arbitrary manner), into stabilizing and overturning components. The spurious nature of the above factor can be proven analytically, since the safety factor is not invariant with respect to the arbitrary choice of the virtual back ω (Fig. 4) (Greco, 1997). It can also be proven that the assumed limit state does not represent the most critical failure mechanism, as the bearing capacity of the footing, or even the structural integrity of the wall, will be exhausted before the wall starts rotating around O. The last remark is recognized in recent codes; however the conventional safety factor against overturning is either preserved (EC7), or replaced by a check of eccentricity of the vertical reaction N on the base of the wall (e.g. AASHTO LRFD, 1994). The above issues are highlighted with the help of following numerical example.

Numerical example

The case of an L-shaped wall with stem width t/H=0.05 and interface roughness $\delta_w=2\phi/3$ retaining soil of unit weight ratio $\gamma/\gamma_w=0.8$ with respect to the unit weight of the wall, friction angle $\phi=35^o$, and slope inclination $\beta=10^o$, is examined. The soil under the wall is assumed to be the same as the retained one. No passive resistance is considered.

In Figures (9a – c), the safety factors against overturning, bearing capacity and sliding are compared for variable heel length and seismic acceleration. In Figure (9d) the corresponding eccentricity of the base reaction is presented for the same cases. It is evident that the safety factor against overturning is always higher than 1, even for cases where the safety factors against sliding and bearing capacity are not satisfied. The significant overtopping of bearing capacity shown in Fig. 9d, is due to the high inclination and high eccentricity of the reaction on the footing, which exceeds the limit of B/6 for a wide range of seismic acceleration coefficients and wall base widths. It can also be noticed that the bearing capacity is overtopped in cases where the eccentricity does not exceed the limit B/3 for dynamic loading according to seismic codes (EC7, EC8).

In Table 1 the corresponding safety factors obtained for different virtual backs ω, are presented. It is evident that the safety factors against sliding and bearing capacity coincide regardless of the arbitrary choice of virtual back, as all possible ω's generate the same reaction at the base of the wall. In contrast, the safety factor against overturning about point O depends on the arbitrary choice of virtual back (angle ω) – a result which is obviously unacceptable.

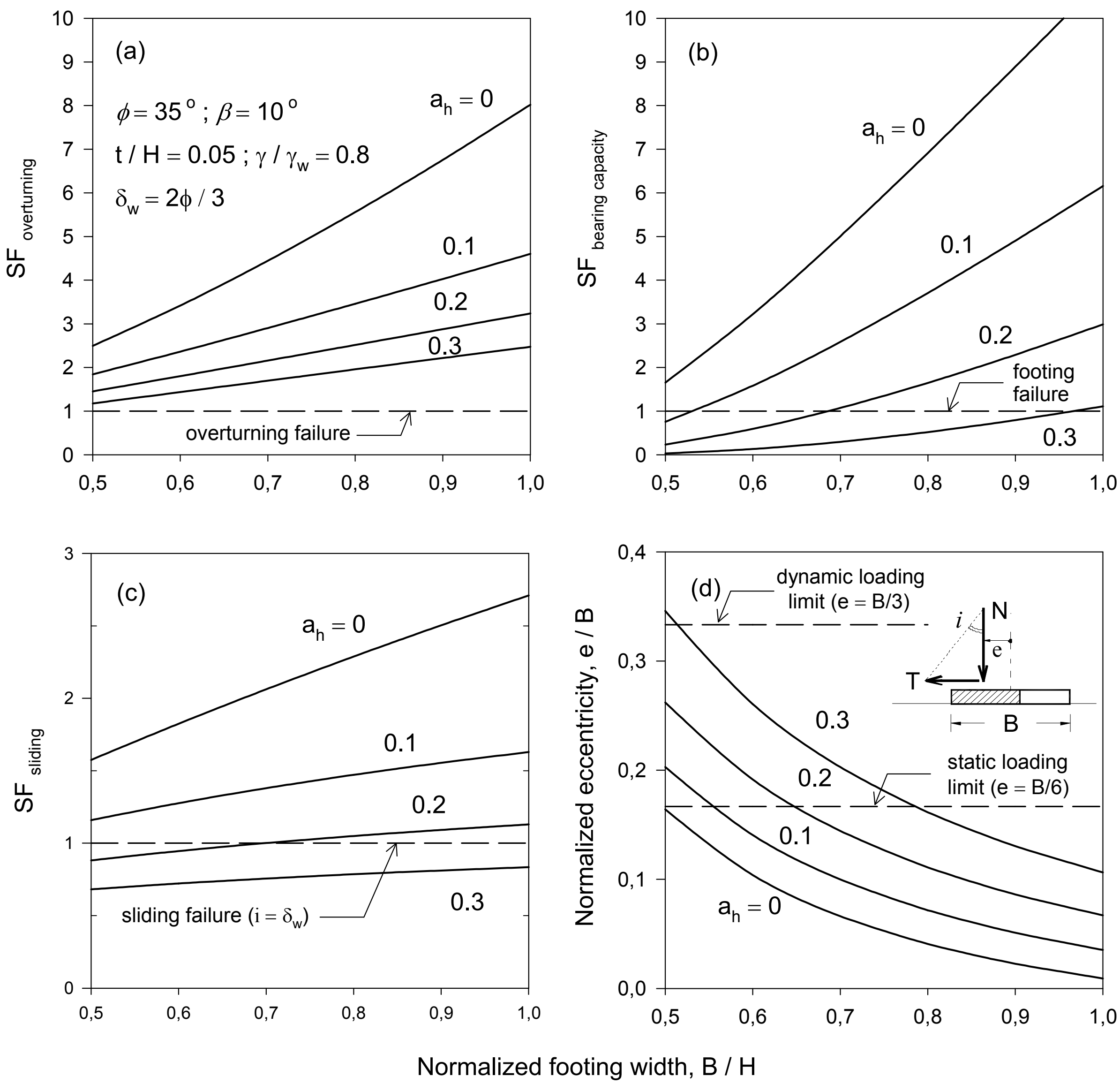

Figure 9. Safety factors against: (a) bearing capacity, (b) overturning, (c) sliding and (d) eccentricity of the contact force, as function of base width and seismic acceleration.

Table 1. Safety factors against sliding, overturning and bearing capacity (ϕ=35^o, δ_w=2ϕ/3, a_h=0.2, B/H=0.8, t/H=0.05, γ/γ_w=0.8).

Arbitrary angle of virtual back, ω (^{o})	$SF_{Sliding}$	$SF_{Overturning}$	$SF_{Bear. Capacity}$
-30	1,05 (all ω's)	2,27	1,65 (all ω's)
-20		2,35	
-10		2,44	
0		2,52	
10		2,60	
20		2,70	
30		2,81	

CONCLUSIONS

An exact analytical solution of the Rankine type was presented for gravitational and earthquake induced earth pressures on L-shaped cantilever retaining walls. The proposed analysis leads to the following conclusions:

1) The geometric condition proposed by some seismic codes for the validity of Rankine condition is not accurate, yet it is satisfactory for a wide range of cases encountered in practice.

2) The active thrust on the wall and the corresponding inclination of the thrust can be determined for any arbitrary virtual back in the backfill. However, the use of the vertical virtual back is advantageous as it leads to simpler geometry. Equations (17) and (18) were derived to determine the active thrust, which are recommended for practical use.

3) The inclination of soil thrust on the vertical virtual back is equal to the slope inclination β only for the case of the gravitational loading (a_h = 0), contrary to the recommendations of a number of seismic codes. However, this spurious assumption yields results on the safe side, with increasing margin of safety under increasing seismic acceleration.

4) The retaining wall stability check may be viewed as a footing stability problem, under an eccentric, inclined load.

5) The conventional safety factor against overturning is defined arbitrarily and does not represent the most critical failure mechanism. It is the opinion of the authors that its use in practice is misleading and should be discontinued.

REFERENCES

AASHTO LRFD (1994), "Bridge Design Specifications", American Association of State Highway and Transportation Officials (AASHTO), Washington, D.C., USA.

Boussinesq, J. (1876)."Essai théoritique sur l'équilibre d'élastité des massifs pulveruients", Mem. Savante etrangere, Acad. Belgique, 40, pp. 1-80.

Budhu, M. (2007), "Soil Mechanics & Foundations", 2nd Edition, J. Wiley & Sons Inc, New York.

BS 8002:1994, Code of Practice for Earth Retaining Structures, B.S. Institution.

Chu, S.C. (1991), "Rankine analysis of active and passive pressures in dry sands", Soils & Foundations, Vol. 31, No. 4, pp.115 – 120.

Clayton, C.R.I., Militisky, J., and Woods, R.I. (1993). Earth Pressure and Earth Retaining Structures, 2nd Edition, Blackie Acad.& Prof.

Costet, J. and Sanglerat, G. (1975). Cours pratique de mechanique des sols, plasticité et calcul des tassements. 2nd edition, Dunod Technique Press, Paris.

EAK 2000 (2003), Greek Seismic Code, OASP, Athens.

Ebeling, R.M., Morrison, E.E., Whitman, R.V., Liam Finn, W.D. (1992). A Manual for Seismic Design of Waterfront Retaining Strutures, US Army Corps of Engineers, Technical Report ITL-92-11.

Eurocode 7, Geotechnical Design, Part 1: General Rules, British Standards Institution, ENV 1997-1.

Eurocode 8, Design provisions for earthquake resistance of structures, Part 5: Foundations, retaining structures and geotechnical aspects, British Standards Institution, ENV 1998-5.

Greco, V.R. (1997), "Stability of Retaining Walls Against Overturning", Journal of Geotechnical & Geoenviromental Engineering, ASCE, Vol. 123, No. 8, pp. 778 – 780.

Greco, V.R. (1999). "Active Earth Thrust on Cantilever Walls in General Conditions", Soils and Foundations, Vol. 39, No. 6, pp. 65–78.

Heyman, J. (1973). "Coulomb's Memoir on Statics; an essay in the history of civil engineering", Cambridge University Press.

Kloukinas, P., Mylonakis, G.E, (2010). "Generalized Rankine Solution for seismic earth pressures" – Submitted for publication.

Kramer, SL (1996). Geotechnical Earthquake Engineering, Prentice Hall.

Levy (1874). "La Statique Graphique et Ses Applications à l'Art des Constructions".

Mylonakis, G.E, Kloukinas, P. and Papantonopoulos, C. (2007). "An alternative to the Mononobe–Okabe equations for seismic earth pressures", Soil Dynamics and Earthquake Engineering, Vol. 27, No. 10, pp. 957-969.

O'Sullivan, C. and Creed, M. (2007). "Using a virtual back in retaining wall design", Geotechnical Engineering, Vol. 160, No. GE3, pp. 147 – 151.

Rankine, W.J.M. (1857). On the stability of loose earth. Philosophical Transactions of the Royal Society of London, Vol. 147, pp. 9 – 27.

Terzaghi, K. (1943). Theoretical soil mechanics, John Wiley & Sons Inc., New York.

Trenter, N.A (2004). "Approaches to the design of cantilever retaining walls", Geotechnical Engineering, Vol. 157, No. 1, pp. 27 – 35.